



1 **Consistency evaluation of tropospheric ozone from ozonesonde and**
2 **IAGOS aircraft observations: vertical distribution, ozonesonde types**
3 **and station-airport distance**

4 Honglei Wang^{1,2}, David W. Tarasick^{3*}, Jane Liu^{2*}, Herman G.J. Smit⁴, Roeland Van Malderen⁵,
5 Lijuan Shen⁶, Tianliang Zhao¹

6 ¹ China Meteorological Administration Aerosol-Cloud and Precipitation Key Laboratory, Nanjing University of
7 Information Science and Technology, Nanjing 210044, China;

8 ²Department of Geography and Planning, University of Toronto, Canada;

9 ³ Environment and Climate Change Canada, 4905 Dufferin Street, Downsview, ON, M3H 5T4 Canada;

10 ⁴ Institute for Energy and Climate Research: Troposphere (IEK-8), Research Centre Juelich (FZJ), Juelich, Germany;

11 ⁵ Royal Meteorological Institute of Belgium, Brussels, Belgium;

12 ⁶ School of Atmosphere and Remote Sensing, Wuxi University, Wuxi 214105, China.

13 * Corresponding authors: David.Tarasick@ec.gc.ca and janejj.liu@utoronto.ca

14

15 **Abstract:** The vertical distribution of tropospheric O₃ from ozonesondes is compared with that from
16 In-service Aircraft for a Global Observing System (IAGOS) measurements at 23 pairs of sites
17 between about 30°S and 55°N, from 1995 to 2021. Profiles of tropospheric O₃ from IAGOS aircraft
18 are in generally good agreement with ozonesonde observations, for Electrochemical concentration
19 cells (ECC), Brewer-Mast, and Carbon-Iodine sensors, with average biases of 7.03 ppb, 6.28 ppb,
20 and -4.48 ppb, and correlation coefficients (R) of 0.72, 0.86, and 0.82, respectively. Agreement
21 between the aircraft and Indian-sonde observations is poor, with an average bias of 24.07 ppb and
22 R of 0.41. The O₃ concentration observed by ECC sondes is on average higher by 5-10% than that
23 observed by IAGOS aircraft, and the relative bias increases modestly with altitude. For other sonde
24 types, there are some seasonal and altitude variations in the relative bias with respect to IAGOS
25 measurements, but these appear to be caused by local differences.

26 The distance between station and airport within 4° has little effect on the comparison results. For
27 the ECC ozonesonde, the overall bias with respect to IAGOS measurements varies from 5.7 to 9.8
28 ppb, when the station pairs are grouped by station-airport distances of <1° (latitude and longitude),
29 1-2°, and 2-4°. Correlations for these groups are R = 0.8, 0.9 and 0.7. These comparison results



30 provide important information for merging ozonesonde and IAGOS measurement datasets. They
31 can also be used to evaluate the relative biases of the different sonde types in the troposphere, using
32 the aircraft as a transfer standard.

33 **Key words:** WOUDC; IAGOS; tropospheric O₃; vertical distribution; ozonesonde; aircraft

34

35 **1 Introduction**

36 Ozone (O₃) is a trace gas with small concentrations in the atmosphere (Ramanathan et al., 1985); it
37 is an important greenhouse gas in the atmosphere. In the planetary boundary layer, it is a major air
38 pollutant (Lefohn et al., 2018; Monks et al., 2015). It can endanger human health, damage
39 ecosystems, and affect climate change (Fu and Tai, 2015; Lefohn et al., 2018; Percy et al., 2003).
40 Therefore, it is of importance to study the temporal and spatial distribution and the factors and
41 mechanisms affecting the variation of tropospheric O₃ including near-surface O₃ (Logan, 1985; Ma
42 et al., 2020; Sharma et al., 2017; Young et al., 2018).

43 A large number of studies have been carried out on the spatiotemporal distribution, formation
44 mechanism, and transport characteristics of ground O₃ (Li et al., 2020, 2021; Vingarzan, 2004; Wang
45 et al., 2017, 2023; Xu et al., 2021; Yu et al., 2021). However, due to the limitation of observations,
46 there are many unknowns on tropospheric ozone, especially the vertical distribution of tropospheric
47 O₃. Satellites provide an effective platform for measuring O₃ globally. Satellite O₃ instruments,
48 including TES, GOME, GOME-2, SCIAMACHY, OMI, and TROPOMI, have been in operation for
49 decades (David et al., 2013; Ebojie et al., 2016; Hegarty et al., 2009; Hoogen et al., 1999; Hubert et
50 al., 2021; Miles et al., 2015). Although satellite observations can provide detailed temporally- and
51 horizontally-resolved maps of tropospheric O₃ columns, in general satellite data lack vertical
52 resolution. While tropospheric differential absorption lidar can also provide vertical distribution
53 information for tropospheric O₃ (Keckhut et al., 2004; Yang et al., 2023), there are very few routinely
54 operating stations.

55 The principal sources of vertically-resolved, trend-quality observations of tropospheric O₃ are
56 therefore balloon-borne ozonesondes, and IAGOS aircraft observations. The World Ozone and
57 Ultraviolet Radiation Data Centre (WOUDC) and the In-service Aircraft for a Global Observing
58 System database (IAGOS) house the data from these two observation programs with the longest



59 duration and the most global stations, which are the most widely used for tropospheric O₃ studies
60 (Gaudel et al., 2020; Liao et al., 2021; Tarasick et al., 2019; Wang et al., 2022). These two datasets
61 are used to study the distribution, variability and trends of tropospheric O₃, and its sources and
62 transport, as well as satellite and model validation (Hu et al., 2017; Gaudel et al., 2018; 2020; Wang
63 et al., 2022; Zhang et al., 2008). The first phase of the Tropospheric Ozone Assessment Report
64 (TOAR-I), initiated in 2014, utilized available surface, ozonesonde, aircraft, and satellite
65 observations to assess tropospheric O₃ trends from 1970 to 2014 (Schultz et al., 2017). Hu et al.
66 (2017) found that the largest bias in a chemical transport model, GEOS-Chem, with respect to
67 ozonesondes and IAGOS observations, is in high northern latitudes in winter-spring, where the
68 simulated ozone is 10-20 ppb lower. Wang et al. (2022) examined observed tropospheric O₃ trends,
69 their attributions, and radiative impacts from 1995 to 2017, using aircraft observations from IAGOS,
70 ozonesondes, and a multi-decadal GEOS-Chem chemical model simulation, and found increases in
71 tropospheric ozone (950 - 250 hPa) of 2.7 ± 1.7 ppbv per decade from IAGOS observations in the
72 Northern Hemisphere and at 19 of 27 global ozonesonde sites averaging 1.9 ± 1.7 ppbv per decade.
73 There are also a number of comparative studies on these two datasets (Zbinden et al., 2013; Staufer
74 et al., 2013, 2014; Tanimoto et al., 2015; Tarasick et al., 2019). Staufer et al. (2013, 2014) used
75 trajectory calculations to match air parcels sampled by both sondes and aircraft. Zbinden et al. (2013)
76 compared coincidences (± 24 hours) at three site pairs, while Tanimoto et al. (2015) examined
77 simultaneous observations (± 3 hours for sonde versus aircraft) at several site pairs less than 100 km
78 apart. In general, these studies show small (6% or less) negative biases of aircraft measurements
79 against ECC sondes. Tarasick et al. (2019) compared trajectory-mapped averages over 20-70 N of
80 ozonesonde and MOZAIC/IAGOS profiles and concluded that over 1994-2012 ozonesonde
81 measurements were about $5 \pm 1\%$ higher in the lower troposphere and $8 \pm 1\%$ higher in the upper
82 troposphere.

83 In this study, we attempt to make the most comprehensive evaluation to date of the relative biases
84 of IAGOS and sonde profiles, using as many station pairs as possible. We identify 23 suitable pairs
85 of sites in the WOUDC and IAGOS datasets from 1995 to 2021, compare the average vertical
86 distribution of tropospheric O₃ shown by ozonesonde and aircraft measurements, and analyze their
87 differences by ozonesonde type and by station-airport distance.



88

89 **2 Data and methods**

90 **2.1 MOZAIC-IAGOS observations**

91 The MOZAIC (Measurements of OZone and water vapor on Airbus In-service airCRAFT) program,
92 initiated in 1994 and incorporated into the IAGOS (In-service Aircraft for a Global Observing
93 System; www.iagos.org) program since 2011, takes advantage of commercial aircraft to provide
94 worldwide in-situ measurements of several trace gases (e.g., O₃ and CO) and meteorological
95 variables (e.g., water vapor) throughout the troposphere and the lower stratosphere (Marenco et al.,
96 1998; Petzold et al., 2015; Nédélec et al., 2015). O₃ measurements are performed using a dual-beam
97 UV-absorption monitor (time resolution of 4 seconds) with an instrumental uncertainty of ± 2
98 ppbv+2% (Thouret et al., 1998; Blot et al., 2021). It should be noted that this is only the instrumental
99 uncertainty, and does not include sampling uncertainties (possible losses) caused by the inlet line
100 and the compressor before the UV-photometric measurements are made. Loss of ozone on the inlet
101 pump was an issue in earlier aircraft ozone sampling programs (Brunner et al., 2001; Dias-Lalcaca
102 et al., 1998; Schnadt Poberaj et al., 2007), but Thouret et al. (1998) found it negligible for
103 MOZAIC/IAGOS.

104 More details on the new IAGOS instrumentation can be found in Nédélec et al. (2015). The
105 continuity of the dataset between the MOZAIC and IAGOS programs has been demonstrated based
106 on their 2-year overlap (2011~2012) (Nédélec et al., 2015). Blot et al. (2021) performed an
107 evaluation of the internal consistency of the O₃ and CO measurements since 1994, which confirmed
108 the instrumental uncertainty of ± 2 ppbv. Moreover they found no drift in the bias amongst the
109 different instrument units (six O₃ and six CO IAGOS-MOZAIC instruments, nine IAGOS-Core
110 Package1 and the two instruments used in the IAGOS-CARIBIC aircraft).

111 **2.2 WOUDC ozonesonde observations**

112 The World Ozone and Ultraviolet Radiation Data Centre (WOUDC) is part of the Global
113 Atmosphere Watch (GAW) program of the World Meteorological Organization
114 (<https://woudc.org/data/explore.php>). The WOUDC is operated by Environment and Climate
115 Change Canada. WOUDC ozonesonde data have been evaluated in a number of WMO-sponsored
116 international field intercomparisons (Attmannspacher and Dütsch, 1970, 1981; Kerr et al, 1994) and



117 more recently in laboratory simulation chamber experiments using a standard reference photometer
118 (Smit et al., 2007, 2024; Thompson et al., 2019). In the global ozonesonde network, while different
119 ozonesonde types were common in the past, more than 95% of current sounding stations use
120 electrochemical concentration cells (ECC). ECC ozonesondes have a precision of 3-5% ($1-\sigma$) while
121 the precision of other sonde types is somewhat poorer, at about 5–10% for Brewer-Mast and the
122 Japanese KC (Carbon-Iodine) sonde, and somewhat larger for the Indian-sonde (Kerr et al., 1994;
123 Smit et al., 2007). Biases with respect to UV reference spectrometers have been estimated for ECC
124 sondes at 1-5% in the troposphere (Smit et al., 2021; Tarasick et al., 2019, 2021).

125 **2.3 Data processing**

126 The two datasets were first screened for airport-sonde station pairs within a latitude separation of
127 $<4^\circ$ and a longitude separation of $<4^\circ$. Many sonde stations have observational records that do not
128 overlap with the IAGOS period (1994-present). In addition, the IAGOS dataset has large gaps at
129 many airports, because the frequency of visits to airports by aircraft that take part in IAGOS depends
130 on commercial airlines' operating constraints. In total, 23 station pairs (Fig. 1) were identified with
131 a separation of less than 4° in both latitude and longitude, and coincident observations over at least
132 nine months. The majority of the 23 ozonesonde site records are ECC (17), while four are Indian-
133 sonde, one Brewer-Mast, and one Carbon-Iodine (the Japanese KC sonde). These stations were
134 divided into 3 groups according to the distance (D) between the ozonesonde station and the airport:
135 $D < 1^\circ$, $1^\circ < D < 2^\circ$, and $2^\circ < D < 4^\circ$. Specific information on the comparison stations is shown in Table
136 1.

137 The observation times of the ozonesonde and aircraft are generally not the same. Ozonesondes are
138 typically launched once a week, although a few stations have more frequent launches. The aircraft
139 records generally contain more frequent observations, but observation times vary. For the selected
140 23 stations, we calculated the mean ozone vertical profiles at 1km resolution (the first layer is from
141 the surface to 1 km above sea level) for each month during the observational period for the two
142 datasets. A minimum of four aircraft profiles were required to estimate a monthly mean profile;
143 because ozonesonde launches are typically only a few times per month, no minimum was required
144 to estimate a monthly mean profile. Only data with monthly means in both datasets were included
145 for further analysis. Comparisons between the two datasets were made by ozonesonde type and by



146 station-airport distance.

147

148 **3. Results and discussion**

149 **3.1 Comparison of the vertical profiles of tropospheric O₃ from four types of ozonesondes and** 150 **aircraft observations**

151 Previous intercomparisons of sondes launched on the same balloon (Attmannspacher and Dütsch,
152 1970, 1981; Beekmann et al, 1994, 1995; Deshler et al., 2008; Hilsenrath et al., 1986; Kerr et al,
153 1994; Smit et al., 2007) have shown that sondes of different types respond somewhat differently to
154 the same ozone profile; that is, they have relative biases, that vary with altitude. Fig. 2 therefore
155 compares the mean vertical profiles of tropospheric O₃ from ozonesonde and aircraft measurements,
156 separated by ozonesonde type. Both O₃ concentrations and absolute differences between
157 ozonesonde and aircraft increase with altitude, especially above 9 km. Average tropospheric O₃
158 profiles observed by ECC, Brewer-Mast, and Carbon-Iodine sondes are in good agreement with
159 aircraft measurements, with biases of 7.03 ppb, 6.28 ppb and -4.48 ppb, respectively, and correlation
160 coefficients (R) of 0.72, 0.86 and 0.82, respectively (Fig. 3a-3c). The Indian-sonde average shows
161 a linear increase with altitude, while the aircraft measurements indicate an ozone decrease with
162 altitude above 8 km (Fig. 2b). This behaviour is most clearly related to the comparisons of stations
163 2°-4° apart in spring (Fig. S8). The agreement between the Indian-sonde and aircraft observations
164 is poor, with a bias of 24.07 ppb, and R of only 0.41 (Fig. 3d). The RMSE of O₃ observed with the
165 four types of ozonesondes (ECC, Brewer-Mast, Carbon-Iodine and Indian-sonde) and the aircraft is
166 small, at 49.15 ppb, 42.08 ppb, 33.55 ppb and 45.90 ppb, respectively.

167 Fig. 2 shows that the mean differences between ozonesonde and aircraft measurements vary
168 significantly with altitude. This can also be observed clearly from the relative differences (RD),
169 expressed as $(O_3\text{-ozonesonde} - O_3\text{-aircraft}) / O_3\text{-aircraft} \times 100\%$ (Fig. 4). O₃ concentrations from ECC
170 measurements are higher than those from aircraft measurements in all altitudes except at the surface.
171 Mean O₃ concentrations reported by Brewer-Mast sondes are lower than those from IAGOS below
172 7 km, but higher between 7 and 12 km. O₃ concentrations reported by Carbon-Iodine sondes are
173 higher than those observed from aircrafts below 2 km, but significantly lower above 8 km. In relative
174 terms, the bias between ECC sonde and aircraft measurements has only a very modest variation



175 with altitude, except near the ground. The mean relative bias for Brewer-Mast measurements is at
176 an absolute maximum of -19 % near the ground, but increases slowly above 3 km, and is positive
177 above 7 km, reaching more than +10 % at 10~11 km. The relative bias for Carbon-Iodine
178 measurements is about 8% below 2 km, is quite small from 2 – 8 km, and becomes large and negative
179 above ~8 km.

180 The Indian-sonde observations show much larger mean differences from the aircraft measurements.
181 Biases are everywhere positive, and as high as nearly 60% or 30 ppb, with much higher uncertainty
182 (standard errors) at each altitude as well (Fig. 2b, Fig. 4).

183 These results are broadly consistent with those from JOSIE 1996 (Smit et al. 1996; Smit and Kley,
184 1998; Thompson et al., 2019), and with the northern hemisphere average result from Tarasick et al.
185 (2019). (Their Figure 20b; note that it is largely based on ECC sondes, and the scale is inverted
186 (IAGOS-sondes) from the sense we use here.)

187 It should be noted that these comparisons only give an average relative bias between sondes and
188 IAGOS. The true value of the ozone profile remains unknown, as do the absolute biases of sondes
189 and IAGOS.

190

191 **3.2 Seasonal dependence of relative biases**

192 Fig. 5 compares mean profiles observed by ECC ozonesondes and IAGOS, separated by season.
193 There are modest seasonal differences in the relative bias profiles, with somewhat larger average
194 biases in winter and spring, but average biases are all positive (ECC sondes higher) and at all levels
195 the average seasonal biases are not statistically different at the 95% confidence level.

196 The modest seasonal differences that are apparent in Fig. 5 and in Figs. S1-S3 are likely due to the
197 modest sample size (for ECC sondes) and small sample sizes (for other types). The actual
198 coincidence in time for profiles can range from less than one day to about 1-3 weeks, depending on
199 the number of ozonesonde and aircraft O₃ profiles collected within each month-bin. This means the
200 larger the atmospheric variability of O₃ is, the larger the real differences between ozonesonde and
201 aircraft O₃ can become, particularly when the number of profiles within a month-bin are small. In
202 addition, there are errors due to variations in the aircraft take-off and landing trajectories and the
203 balloon rise rate, the geographical location of the observation stations (and any associated



204 meteorological differences) and any systematic difference in standard observational times.

205 Table 2 indicates that in all four seasons ECC data correlate well with aircraft observations, with R
206 ranging from 0.71 to 0.76, but with larger average biases in winter and spring, as noted. It is not
207 clear if these seasonal average differences in bias are significant, as the uncertainty ranges on the
208 seasonal averages (lower plot of Fig. 5) overlap.

209 The vertical distribution of tropospheric O₃ observed by Brewer-Mast and IAGOS aircraft in the
210 four seasons is similar (Fig. S1). Differences are also similar, except above 7 km, where the
211 uncertainties are larger, and in general the uncertainty ranges on the seasonal difference averages
212 overlap. Since these comparisons come from only one station pair, some of the differences may be
213 attributable to local differences in topography and meteorology. Table 2 shows that correlations for
214 the ensemble of Brewer-Mast stations are higher than those for ECC stations. Like the ECC sondes,
215 average biases are all positive, but this is determined by the biases above 7 km (Fig. 4); unlike the
216 ECCs, biases are negative in the lowest 3 km.

217 The vertical distribution of tropospheric O₃ concentrations observed by Carbon-Iodine sondes and
218 IAGOS aircraft in the four seasons are similar, except in summer when the tropopause is high (Fig.
219 S2). The difference plots are fairly similar, except in the lowest 3 km, where differences become
220 quite large in summer. Like the previous comparison for Brewer-Mast sondes, these comparisons
221 come from only one station pair, and so the large differences in the boundary layer in summer are
222 likely due to local ozone production sampled by the sonde but not the aircraft. Likely for this reason,
223 the consistency between Carbon-Iodine and aircraft observations is poor in summer, with R being
224 only 0.46 (Table 2). For the other three seasons it is fairly good.

225 The tropospheric O₃ observed by Indian-sondes displays a consistently high bias relative to IAGOS
226 in all seasons, and the seasonal difference plots are quite similar, except in the lowest 3 km in winter
227 (Fig. S3). This different behavior in winter is likely due to local ozone production sampled by the
228 aircraft but not the sonde. Temperature inversions are common in the winter in northern India and
229 trap local pollution. The very low values registered by the aircraft near the surface in summer also
230 suggest local effects, in this case titration by NO_x.

231 Table 2 indicates poor consistency between Indian-sonde and aircraft observations in all four
232 seasons, with R in winter only 0.18.



233 **3.3 Dependence of relative biases on station-airport distances**

234 A major concern with comparing IAGOS and ozonesonde observations is that the stations and
235 airports are not generally co-located, and even where they are close, the flight paths taken by balloon
236 and aircraft are quite different. Fig. 6 compares the average vertical distribution of tropospheric O₃
237 observed at different station-airport distances by ECC sondes and IAGOS aircraft. Note that we
238 continue to separate sonde station data by type --- only ECC data are used here. Sonde-aircraft pairs
239 have been grouped by station-airport distance (Table 1). The differences in average bias vary only
240 very modestly between the different station-airport distance categories, and those differences are
241 not statistically different at the 95% confidence level (Fig. 6d). This, partially owing presumably to
242 the use of mean monthly averages, is encouraging, as this provides further evidence that the average
243 bias we have derived is an artifact strictly of instrument differences.

244 Table 3 indicates that the bias variation between ECC and aircraft observations at different station-
245 airport distances is small, ranging from 5.7 ppb to 9.8 ppb. Correlations for these groupings are also
246 fairly similar, at R = 0.8, 0.9 and 0.7.

247 Compared with ECC sondes, the consistency between the Indian-sonde and aircraft observations is
248 poor at all station-airport distances, with much larger biases, and poor correlations, with R = 0.2 to
249 0.4. Nevertheless, Fig. S4 shows that the profiles of average differences are quite similar for station-
250 airport distances < 1°, and distances of 2°~4° (Fig. S4c).

251 Fig. 7 and Figs. S5-S7 examine possible seasonal variation in the differences at different station-
252 airport distances, for ECC sondes. The mean differences for the different station-airport distance
253 categories are larger than for the annual averages (Fig. 6), but in general those differences are not
254 statistically different at the 95% confidence level (Figs. 7d and S5d-S7d).

255

256 **3.4 Comparison of ozonesonde relative biases under operational conditions using IAGOS**
257 **observations as a transfer standard**

258 The foregoing discussion demonstrates that, consistent with previous work, there is a fairly constant
259 relative bias between IAGOS and sondes, with considerable dependence on sonde type, as expected
260 from previous sonde intercomparisons like JOSIE 1996. Although uncertainties are sizeable due to
261 the relatively sparse nature of the available data, we find consistent differences at all sites, with little



262 dependence on season or on station-airport separation, and little regional dependence (not shown).
263 Notwithstanding this overall sonde-IAGOS bias, we can use these station-airport comparisons to
264 derive relative biases of the different sonde types in use in the global network.

265 This does not assume that the aircraft data are unbiased. The true value of the ozone profile (or even
266 its average) remains unknown, as do the absolute biases of sondes and IAGOS. It does assume:

- 267 1. That the measurement errors are random and normally distributed;
- 268 2. That there is one, constant bias for each measurement type (that is, if, for example, the Indian
269 sonde has changed over the period of comparison, or the IAGOS instruments have different biases,
270 there would be additional error that is not included in our uncertainty estimate);
- 271 3. That the measurement biases are not dependent on the geographic location or other variability of
272 the ozone profile. This does not assume that the average ozone profile is the same, just that the
273 instruments respond in the same way.

274 With these assumptions we can use the results of Fig. 2 to estimate the relative biases of each
275 sonde type to each other. The uncertainty of the comparisons will be the quadratic sum of the
276 uncertainties of the two IAGOS-sonde comparisons. The results are shown in Table 4. This
277 intercomparison of the different sonde types has an important advantage: it compares ozonesonde
278 relative biases under operational conditions, as it compares the data that are actually in databases
279 like the WOUDC. It also fills a gap, as the last WMO international intercomparison involving all
280 four sonde types was JOSIE 1996. These results are broadly consistent with those from JOSIE 1996
281 (Smit and Kley, 1998; their Table 8 and Fig. 11).

282 In fact, the types of ozonesonde have changed during long-term observations at some stations (e.g.
283 Uccle and Payerne). De Backer et al. (1998) showed that with the use of an appropriate correction
284 procedure, accounting for the loss of pump efficiency with decreasing pressure and temperature, it
285 is possible to reduce the mean difference between ozone profiles obtained with both types of sondes
286 below 3%, which is statistically insignificant over nearly the whole operational altitude range (from
287 the ground to 32 km). Stübi et al. (2008) also found that the O₃ difference between the Brewer-Mast
288 and the ECC ozonesonde data shows good agreement between the two sonde types, and the profile
289 of the O₃ difference is limited to ±5% (±0.3 mPa) from the ground to 32 km. The results for Brewer-
290 Mast sondes in Table 4 should also be applicable to the older Payerne and Uccle records, and are



291 generally consistent with these results and with those for the older Canadian records (Tarasick et al.,
292 2002; 2016).

293 The results in Table 4 will be quite valuable for addressing the problem of relative biases when
294 merging ozonesonde data into global climatologies (e.g. McPeters et al., 2007; McPeters and Labow,
295 2012; Bodeker et al., 2013; Liu et al., 2013; Hassler et al., 2018;).

296 **4 Conclusions**

297 The vertical distribution of tropospheric O₃ observed by ozonesondes and IAGOS aircraft sensors
298 are compared at 23 pairs of sites between ~30°S and 55°N from 1995 to 2021. Overall, ECC,
299 Brewer-Mast, and Carbon-Iodine sondes agree reasonably well with aircraft observations, with
300 average biases of 7.03 ppb, 6.28 ppb, and -4.48 ppb, and correlation coefficients of 0.72, 0.86, and
301 0.82, respectively. The agreement between the aircraft and Indian-sonde observations is poor, with
302 an average bias of 24.07 ppb and R of 0.41.

303 Notwithstanding this general agreement, all sonde types show significant average biases with
304 respect to IAGOS. The O₃ concentration observed by ECC sondes is on average higher by 5-10%
305 than that observed by IAGOS aircraft, and the relative bias increases modestly with altitude.
306 Seasonal variations in the relative bias are not in general statistically significant at the 95%
307 confidence level. The distance between station and airport within 4° also has little effect on the
308 comparison results. When the ECC station pairs are grouped by station-airport distances of <1°
309 (latitude and longitude), 1-2°, and 2-4°, biases with respect to IAGOS measurements vary from 5.7
310 to 9.8 ppb, and correlations from 0.7 to 0.9.

311 Thus, the observed average relative bias between sondes and IAGOS found in this study, also noted
312 by previous authors (Zbinden et al., 2013; Staufer et al., 2013, 2014; Tanimoto et al., 2015; Tarasick
313 et al., 2019), is a robust result. Possible reasons for the difference include: side reactions that cause
314 sondes to produce excess iodine (Saltzman and Gilbert, 1959), and/or loss of ozone on the inlet
315 pump that could cause IAGOS monitors to read low at pressures below 800 hPa. The latter was an
316 issue in earlier aircraft ozone sampling programs (Schnadt Poberaj et al., 2007; Dias-Lalcaca et al.,
317 1998; Brunner et al., 2001), but Thouret et al. (1998) found it negligible for MOZAIC/IAGOS.

318 This result implies that care must be taken when merging ozonesonde and IAGOS measurement
319 datasets. While the aircraft and sonde measurements are often complementary, filling in important



320 spatial gaps that would otherwise exist if only one type were used, the records are not typically over
321 the same period, and so merging can introduce spurious jumps if relative biases are not taken into
322 account.

323 The importance of ozone in the troposphere as an air pollutant and a greenhouse gas, and therefore
324 of accurate measurements of its temporal and spatial distribution implies that it will be important to
325 resolve the causes of this bias, and so further research involving more direct comparisons of IAGOS
326 instrumentation and ozonesondes, e.g. in the WCCOS chamber, are strongly recommended.

327 These results are also useful to evaluate the relative biases of the different sonde types in the
328 troposphere, using the aircraft as a transfer standard. This intercomparison of the different sonde
329 types has the advantage that it compares ozonesonde relative biases under operational conditions;
330 that is, the data that are actually in databases like the WOUDC. These results will be invaluable for
331 addressing relative biases when merging ozonesonde data into global climatologies (e.g. Bodeker
332 et al., 2013; Hassler et al., 2018; Liu et al., 2013; McPeters et al., 2007; McPeters and Labow, 2012).

333

334 **Competing interests.** The contact authors have declared that none of the authors has any competing
335 interests.

336 **Data availability.** The global ozone sounding data were acquired from the World Ozone and
337 Ultraviolet Radiation Data Center (<http://www.woudc.org>) operated by Environment Canada. The
338 IAGOS data are created with support from the European Commission, national agencies in Germany
339 (BMBF), France (MESR), and the UK (NERC), and the IAGOS member institutions
340 (<http://www.iagos.org/partners>).

341 **Author contributions.** **HW:** Data curation, Methodology, Validation, Visualization, Writing -
342 original draft preparation, Writing - review & editing, Funding acquisition. **LS:** Methodology,
343 Investigation, Writing - original draft. **DWT:** Data curation, Resources, Conceptualization,
344 Supervision, Writing - original draft preparation, Writing - review & editing. **JL:** Data curation,
345 Resources, Methodology, Conceptualization, Supervision, Writing - original draft preparation,
346 Writing - review & editing, Funding acquisition. **TZ:** Funding acquisition, Writing - review &
347 editing. **HGJS** and **RVM:** Writing - review & editing.

348



349 **Acknowledgments.** We thank many whose dedication makes datasets used in this study possible.
350 The global ozone sounding data were acquired from the World Ozone and Ultraviolet Radiation
351 Data Center (<http://www.woudc.org>) operated by Environment Canada, Toronto, Canada, under the
352 auspices of the World Meteorological Organization. Flight-based atmospheric chemical
353 measurements are from IAGOS. IAGOS is funded by the European Union projects IAGOS-DS and
354 IAGOS-ERI. The IAGOS data are created with support from the European Commission, national
355 agencies in Germany (BMBF), France (MESR), and the UK (NERC), and the IAGOS member
356 institutions (<http://www.iagos.org/partners>). The participating airlines (Lufthansa, Air France,
357 Austrian, China Airlines, Iberia, Cathay Pacific, Air Namibia, Sabena) supported IAGOS by
358 carrying the measurement equipment free of charge since 1994. We are also thankful to the Digital
359 Research Alliance of Canada at the University of Toronto for facilitating data analysis.

360

361 **Financial support.** This study was supported by the Natural Science and Engineering Council of
362 Canada (Grant No. RGPIN-2020-05163), the National Key Research and Development Program of
363 China (Grant No., 2022YFC3701204), the National Natural Science Foundation of China
364 (42275196 and 41830965), the Natural Science Foundation of Jiangsu Province (BK20231300), and
365 Wuxi University Research Start-up Fund for Introduced Talents (2023r035).

366

367 **References**

368 Attmannspacher, A., and Dütsch, H.U., 1970. International ozone sonde intercomparison at the
369 Observatory Hohenpeissenberg, Ber. Dtsch. Wetterdienstes, 120, 1-85.

370 Attmannspacher, A., and Dütsch, H.U., 1981. Second international ozone sonde intercomparison at
371 the Observatory Hohenpeissenberg, Ber. Dtsch. Wetterdienstes, 157, 1-64.

372 Beekmann, M., Ancellet, G., Megie, G., Smit, H.G.J., Kley, D., 1994. Intercomparison campaign of
373 vertical ozone profiles including electrochemical sondes of ECC and Brewer-Mast type and a
374 ground based UV-differential absorption lidar. *Journal of Atmospheric Chemistry*, 19, 259-288.
375 19.

376 Beekmann, M., Ancellet, G., Martin, D., Abonnel, C., Duverneuil, G., Eideliman, F., Bessemoulin,
377 P., Fritz, N., Gizard, E., 1995. Intercomparison of tropospheric ozone profiles obtained by



378 electrochemical sondes, a ground based lidar and an airborne UV-photometer. Atmospheric
379 Environment, 29(9), 1027-1042.

380 Bernhard, G.H., Bais, A.F., Aucamp, P.J., Klekociuk, A.R., Liley, J.B., McKenzie, R.L., 2023.
381 Stratospheric ozone, UV radiation, and climate interactions. Photochemical & Photobiological
382 Sciences, 1-53.

383 Blot, R., Nedelec, P., Boulanger, D., Wolff, P., Sauvage, B., Cousin, J.-M., Athier, G., Zahn, A.,
384 Obersteiner, F., Scharffe, D., Petetin, H., Bennouna, Y., Clark, H., and Thouret, V., 2021.
385 Internal consistency of the IAGOS ozone and carbon monoxide measurements for the last 25
386 years, Atmos. Meas. Tech., 14, 3935-3951, <https://doi.org/10.5194/amt-14-3935-2021>.

387 Bodeker, G. E., Hassler, B., Young, P. J., and Portmann, R. W., 2013. A vertically resolved, global,
388 gap-free ozone database for assessing or constraining global climate model simulations, Earth
389 Syst. Sci. Data, 5, 31-43, <https://doi.org/10.5194/essd-5-31-2013>.

390 Brunner, D., J. Staehelin, D. Jeker, H. Wernli, and U. Schumann, 2001. Nitrogen oxides and ozone
391 in the tropopause region of the Northern Hemisphere: Measurements from commercial aircraft
392 in 1995/96 and 1997, J. Geophys. Res., 106, 27673-27699.

393 Callis, L.B., Boughner, R.E., Natarajan, M., Lambeth, J.D., Baker, D.N. and Blake, J.B., 1991.
394 Ozone depletion in the high latitude lower stratosphere: 1979-1990. Journal of Geophysical
395 Research: Atmospheres, 96(D2), 2921-2937.

396 David, L.M. and Nair, P.R., 2013. Tropospheric column O₃ and NO₂ over the Indian region observed
397 by Ozone Monitoring Instrument (OMI): Seasonal changes and long-term trends. Atmospheric
398 Environment, 65, 25-39.

399 De Backer, H., De Muer, D. and De Sadelaer, G., 1998. Comparison of ozone profiles obtained with
400 Brewer-Mast and Z-ECC sensors during simultaneous ascents. Journal of Geophysical
401 Research: Atmospheres, 103(D16), 19641-19648.

402 Deshler, T., Mercer, J.L., Smit, H.G., Stubi, R., Levrat, G., Johnson, B.J., Oltmans, S.J., Kivi, R.,
403 Thompson, A.M., Witte, J., Davies, J., 2008. Atmospheric comparison of electrochemical cell
404 ozonesondes from different manufacturers, and with different cathode solution strengths: The
405 Balloon Experiment on Standards for Ozonesondes. Journal of Geophysical Research:
406 Atmospheres, 113(D4), D04307, doi:10.1029/2007JD008975.



- 407 Dias-Lalcaca, P., Brunner, D., Imfeld, W., Moser, W. and Staehelin, J., 1998. An automated system
408 for the measurement of nitrogen oxides and ozone concentrations from a passenger aircraft:
409 Instrumentation and first results of the NOXAR project. *Environmental Science & Technology*,
410 32(20), 3228-3236.
- 411 Ebojje, F., Burrows, J.P., Gebhardt, C., Ladstätter-Weißmayer, A., Von Savigny, C., Rozanov, A.,
412 Weber, M. and Bovensmann, H., 2016. Global tropospheric ozone variations from 2003 to 2011
413 as seen by SCIAMACHY. *Atmospheric Chemistry and Physics*, 16(2), 417-436.
- 414 Fu, Y. and Tai, A.P.K., 2015. Impact of climate and land cover changes on tropospheric ozone air
415 quality and public health in East Asia between 1980 and 2010. *Atmospheric Chemistry and*
416 *Physics*, 15(17), 10093-10106.
- 417 García, O.E., Sanromá, E., Schneider, M., Hase, F., León-Luis, S.F., Blumenstock, T., Sepúlveda,
418 E., Redondas, A., Carreño, V., Torres, C. and Prats, N., 2022. Improved ozone monitoring by
419 ground-based FTIR spectrometry. *Atmospheric Measurement Techniques*, 15(8), 2557-2577.
- 420 García, O.E., Schneider, M., Sepúlveda, E., Hase, F., Blumenstock, T., Cuevas, E., Ramos, R., Gross,
421 J., Barthlott, S., Röhlhng, A.N. and Sanromá, E., 2021. Twenty years of ground-based NDACC
422 FTIR spectrometry at Izaña Observatory-overview and long-term comparison to other
423 techniques. *Atmospheric Chemistry and Physics*, 21(20), 15519-15554.
- 424 Gaudel, A., Cooper, O.R., Ancellet, G., Barret, B., Boynard, A., Burrows, J.P., Clerbaux, C., Coheur,
425 P.F., Cuesta, J., Cuevas, E. and Doniki, S., 2018. Tropospheric Ozone Assessment Report:
426 Present-day distribution and trends of tropospheric ozone relevant to climate and global
427 atmospheric chemistry model evaluation. *Elementa: science of the anthropocene*, 6.
- 428 Gaudel, A., Cooper, O.R., Chang, K.L., Bourgeois, I., Ziemke, J.R., Strode, S.A., Oman, L.D.,
429 Sellitto, P., Nédélec, P., Blot, R. and Thouret, V., 2020. Aircraft observations since the 1990s
430 reveal increases of tropospheric ozone at multiple locations across the Northern
431 Hemisphere. *Science Advances*, 6(34), eaba8272.
- 432 Gebhardt, C., Rozanov, A., Hommel, R., Weber, M., Bovensmann, H., Burrows, J.P., Degenstein,
433 D., Froidevaux, L. and Thompson, A.M., 2014. Stratospheric ozone trends and variability as
434 seen by SCIAMACHY from 2002 to 2012. *Atmospheric Chemistry and Physics*, 14(2), 831-
435 846.



- 436 Hassler, B., Kremser, S., Bodeker, G. E., Lewis, J., Nesbit, K., Davis, S. M., Chipperfield, M. P.,
437 Dhomse, S. S., and Dameris, M., 2018, An updated version of a gap-free monthly mean zonal
438 mean ozone database. *Earth System Science Data*, 10, 1473-1490.
- 439 Hegarty, J., Mao, H. and Talbot, R., 2009. Synoptic influences on springtime tropospheric O₃ and
440 CO over the North American export region observed by TES. *Atmospheric Chemistry and*
441 *Physics*, 9(11), 3755-3776.
- 442 Hilsenrath, E., Attmannspacher, W., Bass, A., Evans, W., Hagemeyer, R., Barnes, R., Komhyr, W.,
443 Mauersberger, K., Mentall, J., Proffitt, M., Robbins, D., 1986. Results from the balloon ozone
444 intercomparison campaign (BOIC). *Journal of Geophysical Research: Atmospheres*, 91(D12),
445 13137-13152.
- 446 Hoogen, R., Rozanov, V.V. and Burrows, J.P., 1999. Ozone profiles from GOME satellite data:
447 Algorithm description and first validation. *Journal of Geophysical Research:*
448 *Atmospheres*, 104(D7), 8263-8280.
- 449 Hu, L., Jacob, D.J., Liu, X., Zhang, Y., Zhang, L., Kim, P.S., Sulprizio, M.P. and Yantosca, R.M.,
450 2017. Global budget of tropospheric ozone: Evaluating recent model advances with satellite
451 (OMI), aircraft (IAGOS), and ozonesonde observations. *Atmospheric Environment*, 167, 323-
452 334.
- 453 Hubert, D., Heue, K.P., Lambert, J.C., Verhoelst, T., Allaart, M., Compernelle, S., Cullis, P.D., Dehn,
454 A., Félix, C., Johnson, B.J. and Keppens, A., 2021. TROPOMI tropospheric ozone column data:
455 geophysical assessment and comparison to ozonesondes, GOME-2B and OMI. *Atmospheric*
456 *Measurement Techniques*, 14(12), 7405-7433.
- 457 Keckhut, P., McDermid, S., Swart, D., McGee, T., Godin-Beekmann, S., Adriani, A., Barnes, J.,
458 Baray, J.L., Bencherif, H., Claude, H. and di Sarra, A.G., 2004. Review of ozone and
459 temperature lidar validations performed within the framework of the Network for the Detection
460 of Stratospheric Change. *Journal of Environmental Monitoring*, 6(9), 721-733.
- 461 Kerr, J.B., Fast, H., McElroy, C.T., Oltmans, S.J., Lathrop, J.A., Kyro, E., Paukkunen, A., Claude,
462 H., Köhler, U., Sreedharan, C.R., Takao, T., 1994. The 1991 WMO international ozonesonde
463 intercomparison at Vanscoy, Canada. *Atmosphere-Ocean*, 32(4), 685-716.
- 464 Lefohn, A.S., Malley, C.S., Smith, L., Wells, B., Hazucha, M., Simon, H., Naik, V., Mills, G.,



- 465 Schultz, M.G., Paoletti, E. and De Marco, A., 2018. Tropospheric ozone assessment report:
466 Global ozone metrics for climate change, human health, and crop/ecosystem
467 research. *Elementa: Science of the Anthropocene*, 6.
- 468 Li, K., Jacob, D.J., Liao, H., Qiu, Y., Shen, L., Zhai, S., Bates, K.H., Sulprizio, M.P., Song, S., Lu,
469 X. and Zhang, Q., 2021. Ozone pollution in the North China Plain spreading into the late-
470 winter haze season. *Proceedings of the National Academy of Sciences*, 118(10), e2015797118.
- 471 Li, K., Jacob, D.J., Shen, L., Lu, X., De Smedt, I. and Liao, H., 2020. Increases in surface ozone
472 pollution in China from 2013 to 2019: anthropogenic and meteorological
473 influences. *Atmospheric Chemistry and Physics*, 20(19), 11423-11433.
- 474 Liao, Z., Ling, Z., Gao, M., Sun, J., Zhao, W., Ma, P., Quan, J. and Fan, S., 2021. Tropospheric
475 ozone variability over Hong Kong based on recent 20 years (2000–2019) ozonesonde
476 observation. *Journal of Geophysical Research: Atmospheres*, 126(3), e2020JD033054.
- 477 Liu, G., Liu, J., Tarasick, D.W., Fioletov, V.E., Jin, J.J., Moeini, O., Liu, X., Sioris, C.E. and Osman,
478 M., 2013. A global tropospheric ozone climatology from trajectory-mapped ozone soundings.
479 *Atmospheric Chemistry and Physics*, 13(21), 10659-10675.
- 480 Logan, J.A., 1985. Tropospheric ozone: Seasonal behavior, trends, and anthropogenic
481 influence. *Journal of Geophysical Research: Atmospheres*, 90(D6), 10463-10482.
- 482 Ma, Y., Ma, B., Jiao, H., Zhang, Y., Xin, J. and Yu, Z., 2020. An analysis of the effects of weather
483 and air pollution on tropospheric ozone using a generalized additive model in Western China:
484 Lanzhou, Gansu. *Atmospheric Environment*, 224, 117342.
- 485 McPeters, R.D., Labow, G.J. and Logan, J.A., 2007. Ozone climatological profiles for satellite
486 retrieval algorithms. *Journal of Geophysical Research: Atmospheres*, 112(D5), D05308.
487 doi:10.1029/2005JD006823.
- 488 McPeters, R.D. and Labow, G.J., 2012. Climatology 2011: An MLS and sonde derived ozone
489 climatology for satellite retrieval algorithms. *Journal of Geophysical Research: Atmospheres*,
490 117(D10), D10303. doi:10.1029/2011JD017006.
- 491 Miles, G.M., Siddans, R., Kerridge, B.J., Latter, B.G. and Richards, N.A.D., 2015. Tropospheric
492 ozone and ozone profiles retrieved from GOME-2 and their validation. *Atmospheric
493 Measurement Techniques*, 8(1), 385-398.



- 494 Meng, K., Zhao, T., Xu, X., Zhang, Z., Bai, Y., Hu, Y., Zhao, Y., Zhang, X. and Xin, Y., 2022.
495 Influence of stratosphere-to-troposphere transport on summertime surface O₃ changes in North
496 China Plain in 2019. *Atmospheric research*, 276, 106271.
- 497 Monks, P.S., Archibald, A.T., Colette, A., Cooper, O., Coyle, M., Derwent, R., Fowler, D., Granier,
498 C., Law, K.S., Mills, G.E. and Stevenson, D.S., 2015. Tropospheric ozone and its precursors
499 from the urban to the global scale from air quality to short-lived climate forcer. *Atmospheric*
500 *Chemistry and Physics*, 15(15), 8889-8973.
- 501 Percy, K.E., Legge, A.H. and Krupa, S.V., 2003. Tropospheric ozone: a continuing threat to global
502 forests? *Developments in Environmental Science*, 3, 85-118.
- 503 Perlwitz, J., Pawson, S., Fogt, R.L., Nielsen, J.E. and Neff, W.D., 2008. Impact of stratospheric
504 ozone hole recovery on Antarctic climate. *Geophysical Research Letters*, 35(8).
- 505 Ramanathan, V., Cicerone, R.J., Singh, H.B. and Kiehl, J.T., 1985. Trace gas trends and their
506 potential role in climate change. *Journal of Geophysical Research: Atmospheres*, 90(D3),
507 5547-5566.
- 508 Saltzman, B.E. and Gilbert, N., 1959. Iodometric microdetermination of organic oxidants and ozone.
509 Resolution of mixtures by kinetic colorimetry. *Analytical Chemistry*, 31(11), 1914-1920.
- 510 Schnadt Poberaj, C., Staehelin, J., Brunner, D., Thouret, V. and Mohnen, V., 2007. A UT/LS ozone
511 climatology of the nineteen seventies deduced from the GASP aircraft measurement program.
512 *Atmospheric Chemistry and Physics*, 7(22), 5917-5936.
- 513 Schultz, M.G., Schröder, S., Lyapina, O., Cooper, O.R., Galbally, I., Petropavlovskikh, I., Von
514 Schneidmesser, E., Tanimoto, H., Elshorbany, Y., Naja, M. and Seguel, R.J., 2017.
515 Tropospheric Ozone Assessment Report: Database and metrics data of global surface ozone
516 observations. *Elementa: Science of the Anthropocene*, 5.
- 517 Sharma, S., Sharma, P. and Khare, M., 2017. Photo-chemical transport modelling of tropospheric
518 ozone: A review. *Atmospheric Environment*, 159, 34-54.
- 519 Smit, H.G.J., Sträter, W., Helten, M., Kley, D., Ciupa, D., Claude, H.J., Köhler, U., Hoegger, B.,
520 Levrat, G., Johnson, B., Oltmans, S.J., Kerr, J.B., Tarasick, D.W., Davies, J., Shitamichi, M.,
521 Srivastav, S.K. and Vialle, C., 1996. JOSIE: The 1996 WMO international intercomparison of
522 ozonesondes under quasi-flight conditions in the environmental chamber at Jülich, *Proc.*



- 523 *Quadrennial Ozone Symposium 1996, l'Aquila, Italy*, edited by R. D. Bojkov and G. Visconti,
524 pp. 971-974, Parco Sci. e Tecnol. d'Abruzzo, Italy, 1996.
- 525 Smit, H.G., Straeter, W., Johnson, B.J., Oltmans, S.J., Davies, J., Tarasick, D.W., Hoegger, B., Stubi,
526 R., Schmidlin, F.J., Northam, T., Thompson, A.M., 2007. Assessment of the performance of
527 ECC-ozonesondes under quasi-flight conditions in the environmental simulation chamber:
528 Insights from the Juelich Ozone Sonde Intercomparison Experiment (JOSIE). *Journal of*
529 *Geophysical Research: Atmospheres*, 112(D19), D19306, doi:10.1029/2006JD007308.
- 530 Smit, H.G.J., 2014. Ozonesondes, in *Encyclopedia of Atmospheric Sciences*, Second Edition, edited
531 by G.R. North, J.A. Pyle, and F. Zhang, Vol 1, pp. 372–378, Academic Press, London.
- 532 Smit, H. G. J., Poyraz, D., Van Malderen, R., Thompson, A. M., Tarasick, D. W., Stauffer, R. M.,
533 Johnson, B. J., and Kollonige, D. E., 2023. New insights from the Jülich Ozone Sonde
534 Intercomparison Experiment: calibration functions traceable to one ozone reference instrument.
535 *Atmospheric Measurement Techniques*, 17, 73–112, <https://doi.org/10.5194/amt-17-73-2024>.
- 536 Smit, H.G.J., Thompson, A.M., and the ASOPOS 2.0 Panel, 2021. *Ozonesonde Measurement*
537 *Principles and 1300 Best Operational Practices*, WMO Global Atmosphere Watch Report
538 Series, No. 268, World Meteorological Organization, 1301 Geneva, [Available online at
539 https://library.wmo.int/doc_num.php?explnum_id=10884].
- 540 Solomon, S., 1999. Stratospheric ozone depletion: A review of concepts and history. *Reviews of*
541 *Geophysics*, 37(3), 275-316.
- 542 Staehelin, J., Harris, N.R., Appenzeller, C. and Eberhard, J., 2001. Ozone trends: A review. *Reviews*
543 *of Geophysics*, 39(2), 231-290.
- 544 Staufer, J., Staehelin, J., Stübi, R., Peter, T., Tummon, F., and Thouret, V., 2013. Trajectory matching
545 of ozonesondes and MOZAIC measurements in the UTLS - Part 1: Method description and
546 application at Payerne, Switzerland. *Atmospheric Measurement Techniques*, 6, 3393-3406.
547 doi:10.5194/amt-6-3393-2013.
- 548 Staufer, J., Staehelin, J., Stübi, R., Peter, T., Tummon, F., and Thouret, V., 2014. Trajectory matching
549 of ozonesondes and MOZAIC measurements in the UTLS - Part 2: Application to the global
550 ozonesonde network. *Atmospheric Measurement Techniques*, 7, 241-266. doi:10.5194/amt-7-
551 241-2014.



- 552 Stübi, R., Levrat, G., Hoegger, B., Viatte, P., Staehelin, J. and Schmidlin, F.J., 2008. In-flight
553 comparison of Brewer-Mast and electrochemical concentration cell ozonesondes. *Journal of*
554 *Geophysical Research: Atmospheres*, 113(D13). <https://doi.org/10.1029/2007JD009091>.
- 555 Tanimoto, H., Zbinden, R.M., Thouret, V. and Nédélec, P., 2015. Consistency of tropospheric ozone
556 observations made by different platforms and techniques in the global databases. *Tellus B:*
557 *Chemical and Physical Meteorology*, 67(1), 27073.
- 558 Tarasick, D. W., Davies, J., Anlauf, K., Watt, M., Steinbrecht, W., Claude, H. J., 2002. Laboratory
559 investigations of the response of Brewer-Mast ozonesondes to tropospheric ozone. *Journal of*
560 *Geophysical Research: Atmospheres*, 107(D16), ACH-14,
561 <https://doi.org/10.1029/2001JD001167>.
- 562 Tarasick, D. W., Davies, J., Smit, H. G., Oltmans, S. J., 2016. A re-evaluated Canadian ozonesonde
563 record: measurements of the vertical distribution of ozone over Canada from 1966 to 2013.
564 *Atmospheric Measurement Techniques*, 9(1), 195-214.
- 565 Tarasick, D.W., Galbally, I., Cooper, O.R., Schultz, M.G., Ancellet, G., LeBlanc, T., Wallington, T.J.,
566 Ziemke, J., Liu, X., Steinbacher, M., Stähelin, J., Vigouroux, C., Hannigan, J., Garcia, O., Foret,
567 G., Zanis, P., Weatherhead, E., Petropavlovskikh, I., Worden, H., Neu, J.L., Osman, M., Liu, J.,
568 Lin, M., Granados-Muñoz, M., Thompson, A.M., Oltmans, S.J., Cuesta, J., Dufour, G., Thouret,
569 V., Hassler, B., Thompson, A.M., and Trickl, T., 2019. TOAR- Observations: Tropospheric
570 ozone from 1877 to 2016, observed levels, trends and uncertainties. *Elementa: Science of the*
571 *Anthropocene*, 7(1), 39. DOI: <http://doi.org/10.1525/elementa.376>.
- 572 Tarasick, D.W., Smit, H.G., Thompson, A.M., Morris, G.A., Witte, J.C., Davies, J., Nakano, T., Van
573 Malderen, R., Stauffer, R.M., Johnson, B.J., Stübi, R., Oltmans, S.J., and Vömel, H., 2021.
574 Improving ECC ozonesonde data quality: Assessment of current methods and outstanding
575 issues. *Earth and Space Science*, 8, e2019EA000914. <https://doi.org/10.1029/2019EA000914>.
- 576 Thouret, V., Marenco, A., Logan, J.A., Nédélec, P. and Grouhel, C., 1998. Comparisons of ozone
577 measurements from the MOZAIC airborne program and the ozone sounding network at eight
578 locations. *Journal of Geophysical Research: Atmospheres*, 103(D19), 25695-25720. doi:
579 10.1029/98JD02243.
- 580 Thompson, A. M., Smit, H. G. J., Witte, J. C., Stauffer, R. M., Johnson, B. J., Morris, G., von der



- 581 Gathen, P., Van Malderen, R., Davies, J., Piters, A., Allaart, M., Posny, F., Kivi, R., Cullis, P.,
582 Hoang Anh, N. T., Corrales, E., Machinini, T., da Silva, F. R., Paiman, G., Thiong'o, K., Zainal,
583 Z., Brothers, G. B., Wolff, K. R., Nakano, T., Stübi, R., Romanens, G., Coetzee, G. J. R., Diaz,
584 J. A., Mitro, S., Mohamad, M., and Ogino, S., 2019. Ozonesonde quality assurance: The
585 JOSIE-SHADOZ (2017) experience. *Bull. Am. Meteorol. Soc.*, 100(1), 155-171.
- 586 Vingarzan, R., 2004. A review of surface ozone background levels and trends. *Atmospheric*
587 *environment*, 38(21), 3431-3442.
- 588 Wang, H., Ke, Y., Tan, Y., Zhu, B., Zhao, T. and Yin, Y., 2023. Observational evidence for the dual
589 roles of BC in the megacity of eastern China: Enhanced O₃ and decreased PM_{2.5}.
590 *Chemosphere*, 327, 138548.
- 591 Wang, H., Lu, X., Jacob, D.J., Cooper, O.R., Chang, K.L., Li, K., Gao, M., Liu, Y., Sheng, B., Wu, K.
592 and Wu, T., 2022. Global tropospheric ozone trends, attributions, and radiative impacts in 1995–
593 2017: an integrated analysis using aircraft (IAGOS) observations, ozonesonde, and multi-decadal
594 chemical model simulations. *Atmospheric Chemistry and Physics*, 22(20), 13753-13782.
- 595 Wang, T., Xue, L., Brimblecombe, P., Lam, Y.F., Li, L. and Zhang, L., 2017. Ozone pollution in
596 China: A review of concentrations, meteorological influences, chemical precursors, and
597 effects. *Science of the Total Environment*, 575, 1582-1596.
- 598 Williamson, C.E., Neale, P.J., Hylander, S., Rose, K.C., Figueroa, F.L., Robinson, S.A., Häder, D.P.,
599 Wängberg, S.Å. and Worrest, R.C., 2019. The interactive effects of stratospheric ozone
600 depletion, UV radiation, and climate change on aquatic ecosystems. *Photochemical &*
601 *Photobiological Sciences*, 18(3), 717-746.
- 602 Xu, J., Huang, X., Wang, N., Li, Y. and Ding, A., 2021. Understanding ozone pollution in the
603 Yangtze River Delta of eastern China from the perspective of diurnal cycles. *Science of the*
604 *Total Environment*, 752, 141928.
- 605 Yang, T., Li, H., Wang, H., Sun, Y., Chen, X., Wang, F., Xu, L. and Wang, Z., 2023. Vertical aerosol
606 data assimilation technology and application based on satellite and ground lidar: A review and
607 outlook. *Journal of Environmental Sciences*, 123, 292-305.
- 608 Young, P.J., Naik, V., Fiore, A.M., Gaudel, A., Guo, J., Lin, M.Y., Neu, J.L., Parrish, D.D., Rieder,
609 H.E., Schnell, J.L. and Tilmes, S., 2018. *Tropospheric Ozone Assessment Report: Assessment*



610 of global-scale model performance for global and regional ozone distributions, variability, and
611 trends. *Elementa: Science of the Anthropocene*, 6.

612 Yu, R., Lin, Y., Zou, J., Dan, Y. and Cheng, C., 2021. Review on atmospheric Ozone pollution in
613 China: Formation, spatiotemporal distribution, precursors and affecting
614 factors. *Atmosphere*, 12(12), p.1675.

615 Zang, Z., J.J. Liu, D.W. Tarasick, O. Moeini, B. Jianchun, J. Zhang, R. Van Malderen, A.M. Thompson,
616 H.G.J. Smit, R.M. Stauffer and B.J. Johnson (2024), An updated and improved Trajectory-mapped
617 Ozonesonde dataset for the Stratosphere and Troposphere (TOST) from 1970-2021, to be submitted
618 to ACP.

619 Zbinden, R.M., Thouret, V., Ricaud, P., Carminati, F., Cammas, J.P. and Nédélec, P., 2013. Climatology
620 of pure tropospheric profiles and column contents of ozone and carbon monoxide using MOZAIC
621 in the mid-northern latitudes (24° N to 50° N) from 1994 to 2009. *Atmospheric Chemistry and*
622 *Physics*, 13(24), 12363-12388, <https://doi.org/10.5194/acp-13-12363-2013>, 2013.

623 Zhang, L., Jacob, D.J., Boersma, K.F., Jaffe, D.A., Olson, J.R., Bowman, K.W., Worden, J.R., Thompson,
624 A.M., Avery, M.A., Cohen, R.C. and Dibb, J.E., 2008. Transpacific transport of ozone pollution and
625 the effect of recent Asian emission increases on air quality in North America: an integrated analysis
626 using satellite, aircraft, ozonesonde, and surface observations. *Atmospheric Chemistry and*
627 *Physics*, 8(20), 6117-6136.

628 Zhao, K., Huang, J., Wu, Y., Yuan, Z., Wang, Y., Li, Y., Ma, X., Liu, X., Ma, W., Wang, Y. and Zhang,
629 X., 2021. Impact of stratospheric intrusions on ozone enhancement in the lower troposphere
630 and implication to air quality in Hong Kong and other South China regions. *Journal of*
631 *Geophysical Research: Atmospheres*, 126(18), e2020JD033955.



Figures

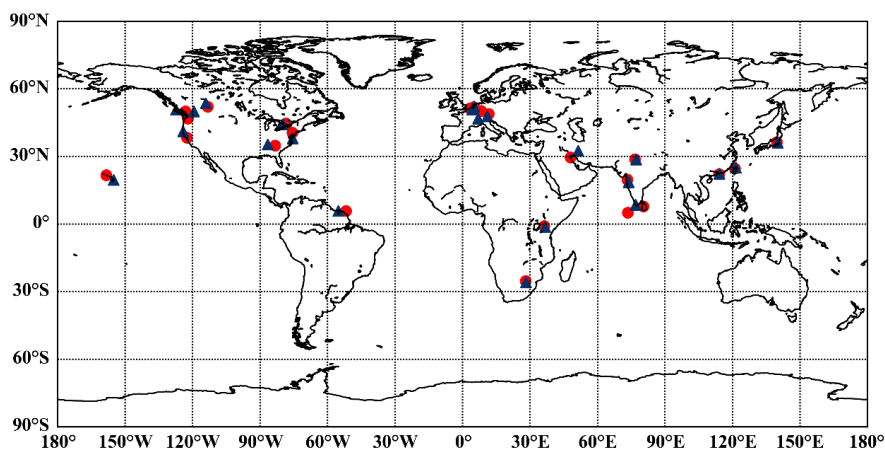


Figure 1. Map of 23 pairs of sites used in this study. Red circle markers are IAGOS sites, blue triangle markers are WUODC sites.

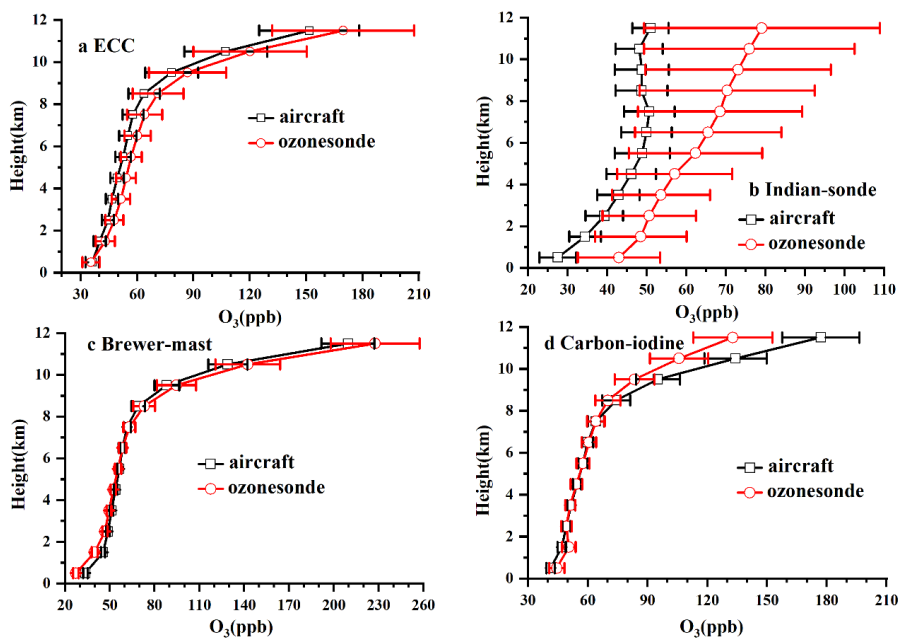


Figure 2. Comparison of the vertical profiles of tropospheric O_3 observed between aircraft measurements and four types of ozonesondes, ECC, Indian-sonde, Brewer-mast, and Carbon-iodine. The error bar length is 4 times the standard error (SE) of the mean (equivalent to 95% confidence limits on the averages).

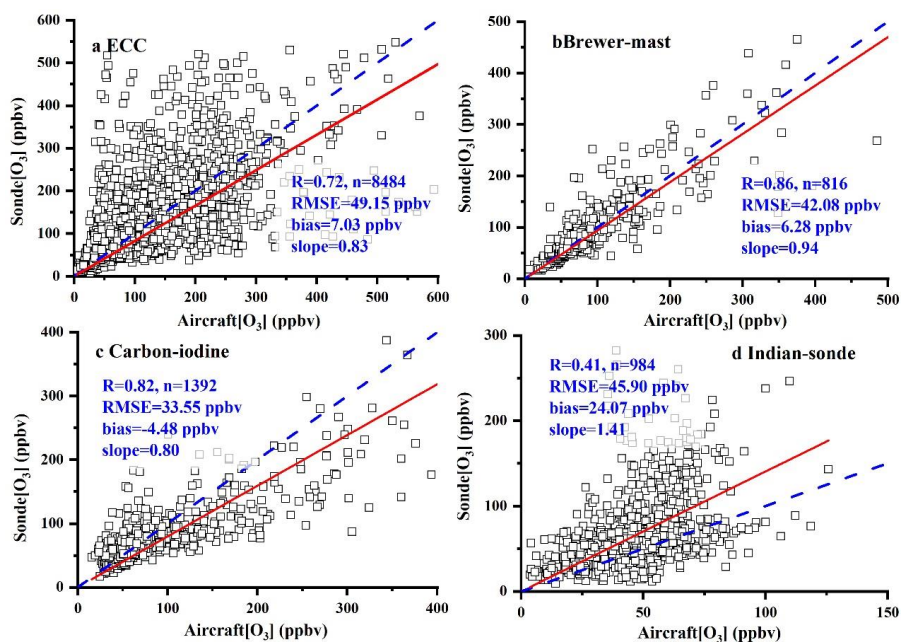


Figure 3. Correlation (R) of ozone mixing ratios between ozonesonde and aircraft measurements.

The blue dashed line shows the 1:1 axis. Correlations are significant at the 99% level ($p < 0.01$). N

denotes the number of data points, and RMSE is the root mean square error.

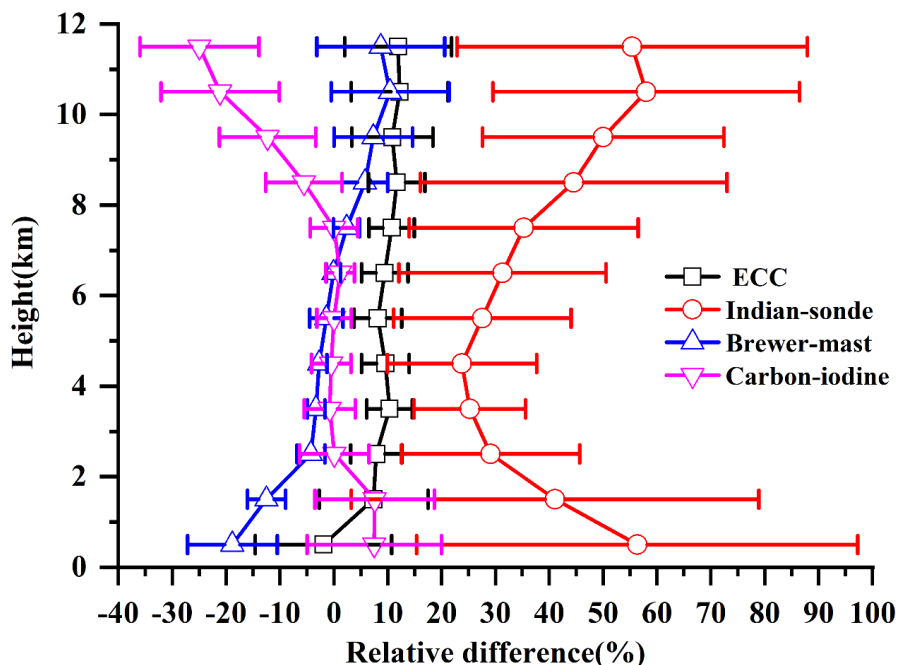


Figure 4. Mean relative difference (RD) between the ozonesonde O_3 and aircraft O_3 data. RD is calculated from $(O_3\text{-ozonesonde} - O_3\text{-aircraft}) / O_3\text{-aircraft} \times 100\%$.

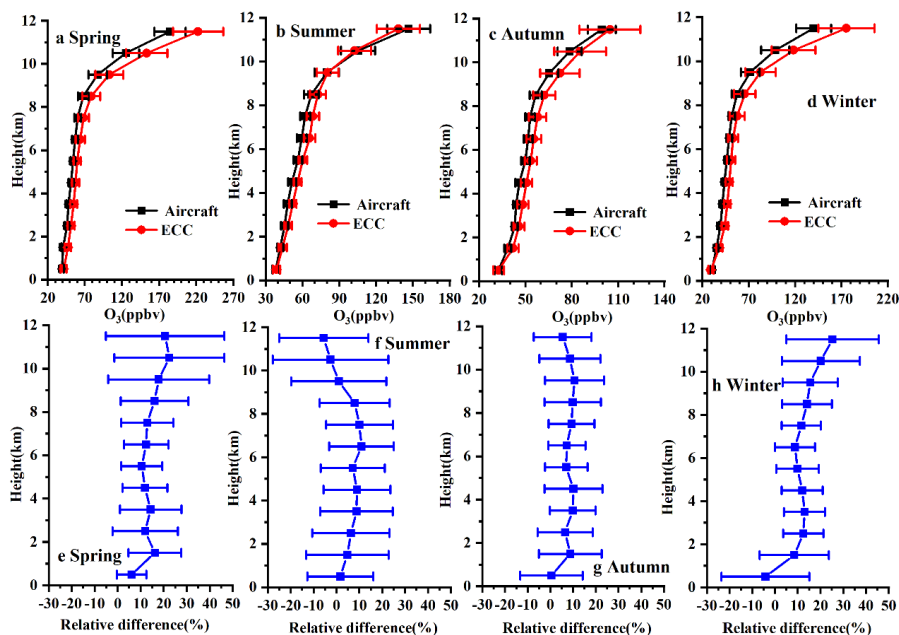




Figure 5. The mean difference in vertical profiles of the tropospheric O₃ between ECC ozonesonde and aircraft observations in four seasons (a-d) and their mean relative difference (e-h).

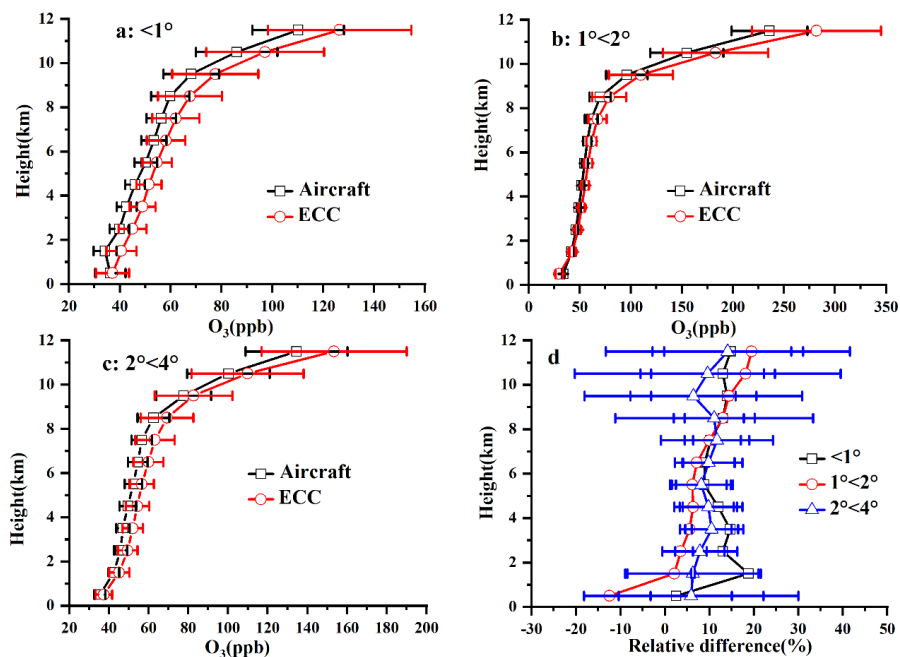


Figure 6. The annual mean vertical profiles of tropospheric O₃ between ECC ozonesonde and aircraft observations at station-pair distances (D) of $D < 1^\circ$ (a), $1^\circ < D < 2^\circ$ (b), and $2^\circ < D < 4^\circ$. The relative differences for the three categories are shown in (d).

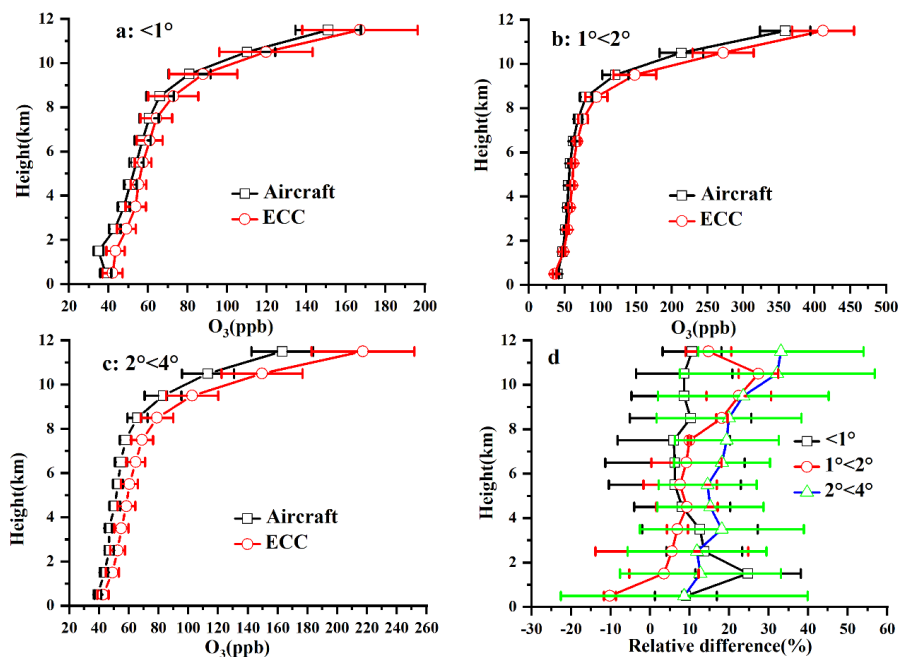


Figure 7. The seasonal mean vertical profiles of tropospheric O₃ in spring between ECC ozonesonde and aircraft observations at station-pair distances (D) of $D < 1^\circ$ (a), $1^\circ < D < 2^\circ$ (b), and $2^\circ < D < 4^\circ$. The relative differences for the three categories are shown in (d).



Tables

Table 1. Summary of the station information, including station's name, geolocation, the number of profiles, observational period, and the station-pair distance used in this study.

MOZAIC-IAGOS				WOUDC				No. valid data months	observation period	station- airport distance
Station name	Lon	Lat	No. profiles	Station name	Lon	Lat	No. profiles			
Toronto	-78.50	44.58	321	Egbert	-79.78	44.23	181	ECC	2004-2008	
Dusseldorf	4.96	51.82	412	De Bilt	5.18	52.10	333	ECC	1995-2013	
Munich	11.63	48.84	2136	Hohenpeissenberg	11.01	47.80	1032	Brewer-mast	1996-2006	
Johannesburg	28.07	-	199	Irene	28.22	25.91	135	ECC	1998-2003	
Nairobi	36.33	-0.94	114	Nairobi	36.75	-1.30	42	ECC	1997-1998	<1°
Mumbai	73.27	19.70	122	Pune	73.85	18.53	56	Indian-sonde	1996-2003	
Delhi	76.65	28.73	342	New Delhi	77.18	28.63	88	Indian-sonde	1995-2016	
Hongkong	114.11	22.10	123	King's Park	114.17	22.31	115	ECC	2000-2005	
Taipei	121.08	24.59	2115	Taipei	121.48	25.02	58	ECC	2014-2018	
Tokyo	139.73	36.33	1342	Tateno (Tsukuba)	140.13	36.05	655	Carbon-iodine	1995-2006	
Calgary	-	52.03	170	Edmonton	-	53.55	112	ECC	2009-2011	1°-2°
Brussels	3.24	51.21	2412	Uccle	4.36	50.80	736	ECC	1997-2009	
Honolulu	-	21.66	169	Hilo (HI)	-	19.58	107	ECC	2015-2017	2°-4°
	158.33				155.07					



Vancouver	-	123.14	49.95	595	Kelowna	-	50.69	594	ECC	68	2003-2015
San-Francisco	-	122.50	38.30	34	Trinidad Head (CA)	-	41.05	53	ECC	10	1999-2001
Portland	-	122.06	46.76	385	Kelowna	119.38	49.97	317	ECC	45	2003-2009
Atlanta	-83.28	34.78	34	34	Huntsville (AL)	-86.58	35.28	85	ECC	10	1999-2006
Washington	-75.59	40.52	610	610	Wallops Island (VA)	-75.46	37.94	616	ECC	80	1994-2014
Cayenne	-51.78	5.75	200	200	Paramaribo	-55.21	5.81	64	ECC	9	2002-2013
Frankfurt	8.30	50.16	12742	12742	Payerne	6.94	46.81	2673	ECC	204	2002-2020
Kuwait-City	48.01	29.52	105	105	Esfahan	51.43	32.48	34	ECC	17	2001-2004
Male	73.49	5.00	76	76	Trivandrum	76.95	8.48	45	Indian-sonde	24	1997-2000
Colombo	80.41	7.79	31	31	Trivandrum	76.95	8.48	37	Indian-sonde	11	1998-2000



1 **Table 2.** Bias, correlation coefficient (R), and RMSE for four types of ozonesonde and aircraft
 2 observations in four seasons.

Type	Season	Bias (O ₃ -ozonesonde - O ₃ -aircraft) (ppb)	R	RMSE (ppb)
ECC	Spring	17.34	0.76	65.52
	Summer	1.96	0.76	40.15
	Autumn	1.75	0.71	34.47
	Winter	7.61	0.71	51.74
Brewer-mast	Spring	10.22	0.94	43.51
	Summer	2.99	0.83	48.79
	Autumn	6.53	0.79	29.40
	Winter	6.11	0.88	45.45
Carbon-iodine	Spring	-9.19	0.84	38.34
	Summer	3.83	0.46	29.31
	Autumn	2.33	0.68	15.10
	Winter	-16.68	0.88	44.72
Indian-sonde	Spring	19.64	0.44	44.30
	Summer	19.58	0.57	37.44
	Autumn	20.38	0.45	37.30
	Winter	40.07	0.18	64.99

3
 4 **Table 3.** Bias, correlation coefficient(R) and RMSE for ECC and Indian-sonde ozonesonde and
 5 aircraft observations at different station-airport distances.

Type	Station-pair distance	Bias (O ₃ -ozonesonde - O ₃ -aircraft) (ppb)	R	RMSE (ppb)
ECC	<1°	9.78	0.78	47.46
	1°~2°	8.91	0.90	40.73
	2°~4°	5.65	0.67	51.00
Indian-sonde	<1°	26.71	0.37	49.54
	2°~4°	15.35	0.24	30.86



6

7 **Table 4.** Comparison of the sondes of each type to IAGOS. (average \pm 2 times the standard error
8 (SE)) Indian-sonde/ECC is (Indian-sonde/IAGOS)/(ECC/IAGOS), Brewer-mast/ECC is (Brewer-
9 mast/IAGOS)/(ECC/IAGOS), Carbon-iodine/ECC is (Carbon-iodine /IAGOS)/(ECC/IAGOS)

Altitude(km)	Indian-sonde/ECC	Brewer-mast/ECC	Carbon-iodine/ECC	ECC/ IAGOS
0~1	1.59 \pm 1.74	0.83 \pm 0.96	1.10 \pm 1.36	0.98 \pm 1.28
1~2	1.31 \pm 1.83	0.81 \pm 0.90	1.00 \pm 1.05	1.07 \pm 1.58
2~3	1.20 \pm 1.62	0.89 \pm 0.97	0.93 \pm 0.85	1.08 \pm 1.54
3~4	1.14 \pm 1.57	0.88 \pm 0.94	0.90 \pm 0.87	1.10 \pm 1.48
4~5	1.13 \pm 1.61	0.89 \pm 1.02	0.91 \pm 0.99	1.10 \pm 1.44
5~6	1.18 \pm 1.76	0.91 \pm 1.05	0.92 \pm 1.04	1.08 \pm 1.37
6~7	1.20 \pm 1.89	0.91 \pm 1.00	0.92 \pm 0.82	1.09 \pm 1.54
7~8	1.22 \pm 1.92	0.92 \pm 0.94	0.90 \pm 0.64	1.11 \pm 1.69
8~9	1.29 \pm 2.09	0.95 \pm 0.99	0.85 \pm 0.55	1.12 \pm 1.61
9~10	1.35 \pm 2.35	0.97 \pm 1.09	0.79 \pm 0.62	1.11 \pm 1.46
10~11	1.41 \pm 3.26	0.98 \pm 1.21	0.70 \pm 0.68	1.12 \pm 1.37
11~12	1.39 \pm 4.61	0.97 \pm 1.19	0.67 \pm 0.72	1.12 \pm 1.42

10

11

12

13